Rotational analysis of the 0_0^0 band of the $\tilde{A}\,^3E$–$\tilde{X}\,^3A_2$ system of methylnitrene

C. R. Brazier and P. G. Carrick
Phillips Laboratory/RKFE, Propulsion Directorate, Edwards Air Force Base, California 93523
P. F. Bernath[a)]
Department of Chemistry, University of Arizona, Tucson, Arizona 85721

(Received 14 May 1991; accepted 2 October 1991)

The optical emission spectrum of the methylnitrene radical has been observed at a resolution of 0.07 cm^{-1}. Transitions to subbands with K up to 3 in the $\tilde{X}\,^3A_2$ ground state were observed and a full rotational analysis carried out. Comparison of the structural information with the highest level theoretical calculations shows agreement to within the estimated error.

INTRODUCTION

The methylnitrene radical (CH_3N) was first observed experimentally just six years ago by Carrick and Engelking.[1] Using both a flowing afterglow discharge and corona excited supersonic expansion (CESE) they obtained the electronic emission spectrum with an origin near 3140 Å. By analogy with the isovalent NH radical, for which the $A\,^3\Pi - X\,^3\Sigma^-$ transition is 3360 Å, the transition was assigned as $\tilde{A}\,^3E - \tilde{X}\,^3A_2$. Theoretical calculations[2] suggest that the singlet states analogous to $a\,^1\Delta$, $b\,^1\Sigma^+$, and $c\,^1\Pi$ for NH have little or no barrier to rearrangement to methyleneimine (CH_2NH), and thus only one electronic system is expected.

A rotationally resolved spectrum of methylnitrene was obtained for the first time by Carrick *et al.*[3] by focusing the emission from a CESE source into the McMath Fourier Transform Spectrometer at Kitt Peak National Observatory. The resolution obtained, about 0.2 cm^{-1}, was sufficient to assign the strongest subband $K' - K'' = 1 - 0$ in the origin systems of both CH_3N and CD_3N. However, even at this resolution and at a temperature of 12 K, the spectral congestion was such that none of the other subbands could be clearly identified.

Other recent experimental studies of methylnitrene include an improved vibrational analysis by Chappell and Engelking[4] and matrix isolation work by Ferrante.[5] In addition, a new theoretical investigation by Xie *et al.*[6] using a large basis set and extensive CI has yielded a ground-state structure much closer to the experimental one, although some discrepancies still remained. We recently recorded a new spectrum using a slit nozzle. Some lines for all the low K subbands 2-3, 1-2, 0-1, 1-0, 2-1, 3-2, and 4-3 were assigned and a full rotational analysis performed. The results of this analysis are presented here.

EXPERIMENTAL

The spectra used in this analysis were obtained in an identical fashion to those obtained previously.[1,3] The first high-resolution data[3] were generated from a pin-hole nozzle and the resolution was limited to 0.2 cm^{-1} by the Doppler spread of the jet. A part of this spectrum is shown in Fig. 1(a). The low resolution severely hampered the analysis because many of the features were composed of two or more rotational lines. Following the work of Milkman *et al.*,[7] we constructed a slot nozzle by drilling a 30 μm by 5 mm channel in the flat end of a glass tube with a pulsed XeCl excimer laser. A discharge jet expansion using such a nozzle dramatically reduces the spread of Doppler velocities of the cooled radicals in the direction of the spectrometer. At the new resolution of 0.07 cm^{-1}, most of the features are resolved into single rotational lines as can be seen in Fig. 1(b).

The corona jet source tends to remain stable for only short periods of time, so several separate scans were recorded. Of these scans, two were used in the analysis; the first

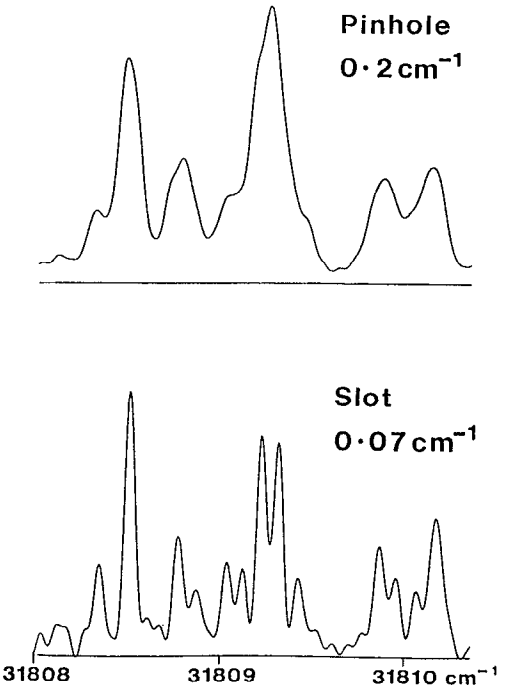

FIG. 1. Comparison of the methylnitrene emission spectra obtained from pin-hole and slot-type nozzles. The Doppler width of the lines is reduced dramatically from 0.2 cm^{-1} full width at half maximum to 0.07 cm^{-1}. At the higher resolution most of the lines are well resolved making assignment of branches much easier.

[a)] Also at: Department of Chemistry, University of Waterloo, Waterloo, Ontario, Canada N2L 3G1.

 0021-9606/92/020919-08$06.00

resulted in a strong spectrum with a rotational temperature of about 12 K. This was used to make initial assignments of the line positions. A second spectrum with a rotational temperature of 25 K made possible the tracking of branches to higher rotational quantum number J. As a result, some of the centrifugal distortion constants could be determined.

ANALYSIS

Initially the 1-0 subband which had previously been analyzed using a $^3\Pi - {}^3\Sigma^-$ Hamiltonian[2] was reanalyzed using a $^3E - {}^3A_2$ Hamiltonian. As no transition of this type had been analyzed before, the effective Hamiltonian for a ^3E electronic state had to be developed. The starting point was the ^2E Hamiltonian of Endo *et al.*[8] which we had previously used and extended for the analysis of the $^2E - {}^2A_1$ transition of $CaCH_3$.[9] The only additional terms required are the spin–spin interaction λ and the rovibronic interaction terms o_1 and o_2 analogous to the lambda doubling parameter o for a $^3\Pi$ state. The effective Hamiltonian and matrix elements for a ^3E state are given in the Appendix.

The arrangement of the K stacks for CH_3N is shown in Fig. 2. They are grouped in columns by K_R, the rotational angular momentum about the top axis. This makes it easier to visualize the allowed rotational transitions as they only occur within columns ($K'_R - K'' = 0$). The rotational angular momentum without spin is then $K = K_R \pm 1$. Strictly speaking, all of these terms are signed, and in the absence of ro-vibronic coupling, every level except for $K = 0$ in the $\tilde{X}\,^3A_2$ ground state is a degenerate pair. For a given value of K_R ($\neq 0$) there are 12 possible basis functions as K_R and ζ can be plus or minus and each of the four resulting K levels can couple with the spin angular momentum Σ (-1, 0, or 1) to give 12 possible values for the projection of the total angular momentum P on the top axis. ζ is the projection of the orbital angular momentum on the symmetry axis, analagous to the quantum number Λ of a diatomic molecule. The quantum number P corresponds to Ω in the diatomic case.

For example, the basis functions for $|K_R| = 3$ are

$$|J,\ \zeta = 1,\ K = 4,\ P = 5,\ \Sigma = 1\rangle,$$
$$|J,\ \zeta = 1,\ K = 4,\ P = 4,\ \Sigma = 0\rangle,$$
$$|J,\ \zeta = 1,\ K = 4,\ P = 3,\ \Sigma = -1\rangle,$$
$$|J,\ \zeta = -1,\ K = 2,\ P = 3\ \Sigma = 1\rangle,$$
$$|J,\ \zeta = -1,\ K = 2,\ P = 2,\ \Sigma = 0\rangle,$$
$$|J,\ \zeta = -1,\ K = 2,\ P = 1\ \Sigma = -1\rangle,$$
$$|J,\ \zeta = -1,\ K = -4,\ P = -3,\ \Sigma = 1\rangle,$$
$$|J,\ \zeta = -1,\ K = -4,\ P = -4,\ \Sigma = 0\rangle,$$
$$|J,\ \zeta = -1,\ K = -4,\ P = -5,\ \Sigma = -1\rangle,$$
$$|J,\ \zeta = 1,\ K = -2,\ P = -1,\ \Sigma = 1\rangle,$$
$$|J,\ \zeta = 1,\ K = -2,\ P = -2,\ \Sigma = 0\rangle,$$
$$|J,\ \zeta = 1,\ K = -2,\ P = -3,\ \Sigma = -1\rangle.$$

Following Endo *et al.*[8] we take parity combinations and represent each pair by the value of K for the basis function with $\zeta = 1$:

$$|J,K,P,\Sigma;\pm\rangle = \frac{1}{\sqrt{2}}\,[\,|J,\zeta = 1,P,\Sigma\rangle \pm (-1)^{J-P-\Sigma+1}|J,\zeta = -1,-P,-\Sigma\rangle\,].$$

The six parity combinations are then

$$|J,\ K = 4,\ P = 5,\ \Sigma = 1,\pm\rangle,$$
$$|J,\ K = 4,\ P = 4,\ \Sigma = 0,\pm\rangle,$$
$$|J,\ K = 4,\ P = 3,\ \Sigma = -1,\pm\rangle,$$
$$|J,\ K = -2,\ P = -1,\ \Sigma = 1,\pm\rangle,$$
$$|J,\ K = -2,\ P = -2,\ \Sigma = 0,\pm\rangle,$$
$$|J,\ K = -2,\ P = -3,\ \Sigma = -1,\pm\rangle.$$

Initially only the (2,2) interaction terms[8] between K levels were included. These terms connect the two K levels which arise from a given K_R, for example, $K = 4$ and -2 from $|K_R| = 3$. In the case of $K = 1$, the (2,2) terms lift the degeneracy of the two parity combinations and are analogous to Λ type doubling in a linear molecule. The advantage of this restriction is that it keeps the Hamiltonian matrices to a manageable size, a maximum dimension of 6×6.

For the final analysis the $(2, -1)$ terms[8] were also included, but these link across K_R stacks connecting all K levels of a given spin symmetry. For the observed e symmetry levels ($K' = 0,2,-1,3$), the next set of connecting levels

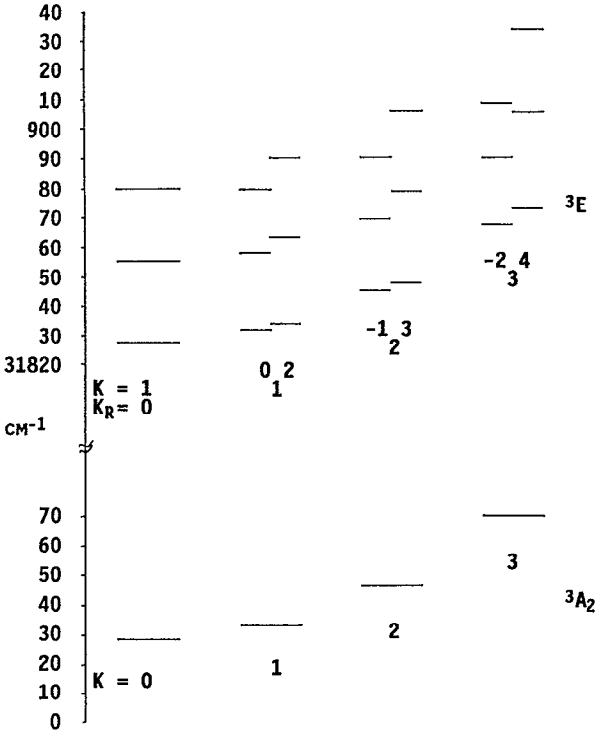

FIG. 2. Energy-level diagram for methylnitrene showing the arrangement of the K stacks and the splitting of the ^3E state into separate spin-orbit components. This is an inverted ^3E state, so $\Omega = 2$ lies lowest and $\Omega = 0$ highest. For each K stack, the level with $J = 5$ is shown because this is the first level which occurs for all the K stacks shown. Excited state perturbations can occur between levels (1 and 2) for which $K_1 + K_2 = -1$, for example, $K = 0$ with $K = -1$.

($K' = -3,5, -4,6$) were included and all higher energy states ignored, giving a 24×24 matrix. For the a_1 and a_2 symmetry levels ($K = 1, -2,4$) the next set ($K = -5,7$) was similarly included giving a 15×15 matrix. The $(2, -1)$ terms can give rise to significant perturbations when different K levels pass through each other. Such effects are very useful in a symmetric top molecule because they determine the separation of the K stacks. Ordinarily, the spacing of the K stacks cannot be determined and, hence, the absolute value of the A rotational constant is difficult to measure. In a few molecules, such as CH_3F[10] perturbations due to low lying vibrations have allowed the determination of A. For a ^2E or ^3E state there is the possibility of different spin-orbit components of separate K levels lying close in energy and interacting, as can be seen in Fig. 2. A perturbation of this type was seen for $CaCH_3$,[9] and the value of A determined. Unfortunately, for CH_3N, only a few low J and low K levels have been seen and no perturbations of this type were observed. However, these terms effect the energy levels even when the K levels are not close together, and if the data is sufficiently good, A can be determined. This was done for CH_3O,[8] where very high precision microwave data was available.

In the case of methylnitrene, when both A rotational constants were allowed to vary, the absolute value could only be determined to 0.4 cm^{-1}. When A'' was constrained in the least-squares fit and adjusted manually, a gentle minimum at $A'' = 5.61$ cm^{-1} was found. The Fourier transform (FT) data for CH_3N probes primarily low J and K levels in the $\Omega = 2$ stack of the ^3E state. Some lines from the $\Omega = 1$ levels were seen in the higher temperature emission spectrum allowing the spin–orbit splitting to be determined. Some transitions were also seen in the region of the $\Omega = 0$ component, but these were overlapped by a vibrational hot band. The structure of this band is very different from that of the origin suggesting that it originates from one of the e vibrational levels in the excited state. As 6_1^1 has already been assigned,[4] this leaves 4_1^1 and 5_1^1 as the most likely assignments.

It should be noted that the transitions from the $\Omega' = 1$ component were incorrectly assigned as being from $\Omega' = 2$ to $\Omega'' = \pm 1$ in the ground state by Chappell and Engelking.[4] The ground state has a very small splitting and follows Hunds' case (b) coupling where Ω has no meaning.

The only data for $\Omega = 0$ in the ^3E state are from laser-induced fluorescence (LIF) measurements reported previously.[3] Comparison of the emission spectra and LIF spectra for the $\Omega = 2$ and 1 components shows that the LIF data are subject to random errors of up to 0.05 cm^{-1}. Such errors were expected because the scan to scan reproducibility of the LIF signals was typically of this size. The shifts were produced by variations in the direction of flow of the nozzle resulting in different Doppler shifts. This could be overcome if the experiments were repeated using a slot nozzle.

For the final fit, 247 FT lines and 8 LIF transitions were included; these are listed in Table I together with residuals. The transitions observed spanned rotational levels up to $J = 13$ for $K'' = 0$, 1, 2, and 3. The ground state could be fitted adequately with just four adjustable parameters: B, D_N, λ, and $(\epsilon_{bb} + \epsilon_{cc})/2$ as can be seen in Table II. For the excited state, many more parameters were required to obtain a satisfactory fit. Inclusion of the $(2, -1)$ terms connecting the K stacks improved the variance from 0.95 to 0.90. Several other higher-order terms such as D_{NK} and η_e were also required. The values for these parameters are poorly determined and subject to significant variation depending on the particular group of parameters selected to fit the data.

DISCUSSION

The ground-state rotational constant $B = 0.9296$ cm^{-1} found from fitting the electronic emission data to a $^3E - {}^3A_2$ Hamiltonian, is changed little from the earlier fit[3] of the 1-0 subband to a $^3\Pi - {}^3\Sigma^-$ Hamiltonian (0.9308 cm^{-1}). As the value of the A rotational constant could not be reliably determined, calculation of the geometry depends on fixing the structure of the methyl group. Using the new theoretical values of Xie *et al.*[6] (see Table III) gives $r_{C-N} = 1.420$ Å in good agreement with the theoretical value of 1.424 Å. Using the experimental bond angle[3] determined from B rotational constants for CH_3N and CD_3N gives $r_{C-N} = 1.412$ Å; essentially the same as the earlier experimental value. The CD_3N molecule has not yet been reanalyzed using a $^3E - {}^3A_2$ Hamiltonian, so it is not possible to make a reliable comparison between isotopomers using the new data.

In view of the fact that the theoretical calculations give a bond angle near 109° at all levels of theory, it is likely that the value for the H–C–H bond angle, estimated earlier[3] is too low. This is most likely due to zero-point vibrational contributions to the rotational constants of CD_3N and CH_3N which affect the precision of structure estimates based on isotopic substitution.[11] An accurate determination of the A rotational constant is required to definitively solve this problem. This could be obtained either from microwave observations or further LIF experiments to probe the levels which are predicted to exhibit internal perturbations due to the crossing of levels of different Ω and K.

The $\tilde{X}\,^3A_2$ ground state of CH_3N could be fitted adequately with just four adjustable parameters, while a total of sixteen were required for the excited state. In addition, the centrifugal distortion constant D_N was at least a factor of 5 smaller in the $\tilde{A}\,^3E$ state than in the ground state, although a reliable D_N value could not be determined. This suggests the presence of either some internal or external perturbation interaction which makes the energy levels hard to describe by a conventional effective Hamiltonian. In the relatively small number of levels probed at high precision, no obvious local perturbations were seen. The majority of the lines observed were very weak and, hence, not determined precisely enough to spot small perturbations.

Some information on the Jahn–Teller interaction in the $\tilde{A}\,^3E$ state can be extracted from the experimental parameters. From the values of A and $A\zeta_t$ the total angular momentum projected on the top axis ζ_t was found to be 0.603. The observed spin–orbit splitting, $a\zeta_e d$ is -22.52 cm^{-1}. The unquenched spin–orbit splitting, a, can be estimated to be the same as that for NH, $A(=a) = -34.62$ cm^{-1} (Ref. 12) giving $\zeta_e d = 0.65$.

TABLE I. Observed lines of methylnitrene (in cm^{-1}).

J	1-0 subband											
	$P_1(J)$		$Q_1(J)$		$R_1(J)$		$P_{12}(J)$		$Q_{12}(J)$		$R_{12}(J)$	
1					31 809.2279	−0.0020					31 806.6719	0.0004
2			31 807.4442	0.0044	31 812.2077	0.0009			31 802.9568	0.0031	31 807.7217	−0.0002
3	31 803.7585	0.0061	31 808.5198	−0.0008	31 814.8808	0.0005	31 797.3731	−0.0048	31 802.1442	−0.0007	31 808.5092	0.0007
4	31 802.9568	−0.0049	31 809.3197	−0.0057	31 817.2801	−0.0000	31 794.7129	0.0013	31 801.0730	0.0017	31 809.0359	0.0003
5	31 801.9003	−0.0005	31 809.8677	0.0025	31 819.4195	0.0020	31 791.7858	0.0038	31 799.7364	−0.0004		
6	31 800.5796	0.0035			31 821.3035	0.0036			31 798.1380	−0.0081		
7	31 798.9929	−0.0006			31 822.9422	0.0082	31 785.1627	0.0106	31 796.3037	−0.0006	31 809.1149	0.0006
8					31 824.3401	0.0141	31 781.4711	0.0079	31 794.2182	0.0010	31 808.6586	−0.0012
9							31 777.5296	−0.0034	31 791.8958	0.0054		
10			31 808.8519	0.0105			31 773.3795	0.0113	31 789.3214	−0.0088		
11	31 790.1947	−0.0068	31 807.9353	−0.0031					31 786.5418	−0.0006	31 805.9361	−0.0052
12			31 806.8139	−0.0036					31 783.5303	−0.0029		
13	31 784.4050	−0.0090	31 805.4839	−0.0007					31 780.3009	−0.0072		
	$P_{13}(J)$		$Q_{13}(J)$		$R_{13}(J)$		$P_{21}(J)$		$Q_{21}(J)$		$R_{21}(J)$	
1					31 803.9615	0.0005			31 832.4949	−0.0017	31 835.8147	−0.0000
2			31 798.3175	0.0009	31 803.0746	−0.0090			31 834.0701	0.0094	31 839.0438	0.0141
3			31 795.6190	−0.0010	31 801.9697	−0.0100	31 830.3467	0.0095	31 835.4019	−0.0103	31 842.0227	0.0011
4	31 786.3052	−0.0034	31 792.6708	−0.0015	31 800.6156	−0.0115	31 829.7847	0.0001	31 836.5660	−0.0078	31 844.8306	0.0104
5			31 789.4749	0.0036	31 799.0339	0.0102	31 829.0394	−0.0027	31 837.5460	−0.0073	31 847.4266	−0.0094
6	31 776.4486	0.0003							31 838.3544	0.0000	31 849.8629	−0.0121
7			31 782.3347	0.0118					31 838.9721	−0.0070		
8			31 778.3923	0.0065					31 839.4339	0.0052		
9			31 774.2244	0.0096								
	$P_{23}(J)$		$Q_{23}(J)$		$R_{23}(J)$		$Q_{31}(J)$		$Q_{32}(J)$		$R_{32}(J)$		$Q_{31}(J)$
1			31 827.2385	0.0108	31 830.5637	0.0179	31 857.014	0.041	31 850.800	0.021	31 858.010	−0.017	
2	31 821.5782	0.0075	31 824.9546	0.0171	31 829.9015	−0.0050	31 858.798	0.002	31 850.700	0.009	31 859.726	0.003	
3	31 817.4278	−0.0088	31 822.5049	−0.0067	31 829.1102	−0.0108	31 860.520	−0.001	31 850.511	−0.039			
4	31 813.1382	0.0066	31 819.9272	0.0064			31 862.130	−0.041	31 850.344	−0.004			
5	31 808.6586	0.0103	31 817.1624	0.0029					31 850.077	0.000			
6			31 814.2256	−0.0010					31 849.727	−0.001			
7			31 811.1184	−0.0036					31 849.298	0.007			
8													
9			31 804.4039	0.0053									

TABLE I. (*Continued.*)

0-1 subband

	$P_1(J)$		$Q_1(J)$		$R_1(J)$		$P_{12}(J)$		$Q_{12}(J)$		$R_{12}(J)$	
1											31 806.8456	0.0017
2			31 806.4230	0.0077	31 811.1775	0.0170	31 799.2049	− 0.0035	31 802.3667	− 0.0030	31 807.1140	− 0.0009
3			31 807.5579	0.0051	31 813.8855	− 0.0001	31 796.6572	0.0076	31 801.3886	− 0.0062		
4			31 808.3503	− 0.0074	31 816.2863	0.0036	31 793.9033	− 0.0001	31 800.2391	0.0029	31 808.1459	− 0.0153
5	31 800.9654	0.0145	31 808.8722	− 0.0037	31 818.3898	− 0.0087	31 790.9128	− 0.0027	31 798.8371	− 0.0034		
6	31 799.5924	− 0.0094					31 787.6649	− 0.0096				
7							31 784.1783	− 0.0021	31 795.3105	0.0042		
8							31 780.4363	− 0.0004	31 793.1697	− 0.0025		
9							31 776.4499	0.0008	31 790.8177	0.0174		
10							31 772.2345	0.0108	31 788.1999	0.0032		
11							31 767.7745	0.0074				

	$P_{13}(J)$		$Q_{13}(J)$		$R_{13}(J)$		$P_{21}(J)$		$Q_{21}(J)$		$R_{21}(J)$	
1			31 799.5879	0.0021	31 802.7400	− 0.0071						
2	31 794.1376	− 0.0142	31 797.3197	0.0066	31 802.0512	− 0.0071			31 831.280	0.009	31 836.271	− 0.009
3	31 789.9206	0.0076	31 794.6670	0.0088	31 799.6281	0.0045			31 832.660	− 0.013	31 839.354	− 0.004
4	31 785.3831	0.0083	31 791.7029	− 0.0047	31 798.0081	0.0016	31 827.128	− 0.017	31 833.817	− 0.013	31 842.181	− 0.013
5	31 780.5537	− 0.0052	31 788.4812	− 0.0027			31 826.416	− 0.007	31 834.780	− 0.007		
6	31 775.4564	− 0.0190	31 784.9778	− 0.0202			31 825.503	− 0.010	31 835.576	0.017		
7			31 781.2497	− 0.0083			31 824.424	0.001	31 836.166	0.011		
8												
9												

	$Q_2(J)$		$P_{23}(J)$		$Q_{23}(J)$		$R_{23}(J)$	
1							31 827.624	0.022
2								
3					31 819.761	− 0.017	31 826.461	− 0.002
4					31 817.162	− 0.018		
5			31 806.021	− 0.010	31 814.391	− 0.004	31 824.424	− 0.017
6	31 823.622	− 0.010			31 811.458	0.025		
7	31 822.343	− 0.004	31 796.600	0.033				
8			31 791.603	0.026				
9			31 786.433	0.013				

2-1 subband

	$Q_1(J)$		$R_1(J)$		$R_{12}(J)$		$R_{21}(J)$	
2			31 812.8164	− 0.0002	31 808.7743	0.0033	31 841.352	− 0.004
3			31 815.5944	0.0003	31 809.4363	0.0003		
4	31 810.0623	− 0.0039	31 818.0506	− 0.0034				
5	31 810.6449	− 0.0022	31 820.2427	0.0014				
6	31 810.9376	− 0.0297	31 822.1670	− 0.0052				
7	31 811.0296	− 0.0062						
8	31 810.8579	− 0.0020						

TABLE I. (*Continued.*)

1-2 subband

	$P_{12}(J)$		$Q_{12}(J)$		$P_{13}(J)$		$Q_{13}(J)$	
1					31 796.4045	0.0134		
2					31 792.8574	0.0107	31 795.9819	− 0.0066
3	31 796.1016	− 0.0010			31 788.7505	0.0108	31 793.4556	− 0.0008
4					31 784.2305	− 0.0154	31 790.5521	0.0100
5								
6			31 796.1959	0.0150			31 783.7919	− 0.0094
7								
8			31 792.0146	0.0214				

3-2 subband

	$Q_1(J)$		$R_1(J)$		$R_{12}(J)$		$R_{21}(J)$	
3			31 815.9982	0.0020	31 810.5017	− 0.0098	31 846.460	− 0.018
4	31 810.5705	− 0.0011	31 818.5902	0.0078	31 810.8645	0.0095		
5	31 811.2316	0.0089	31 820.8371	− 0.0063	31 811.0686	− 0.0002		
6	31 811.5917	− 0.0037	31 822.8342	0.0047				
7	31 811.7174	0.0082	31 824.5648	0.0040				
8			31 826.0484	− 0.0003				

2-3 subband

	$P_1(J)$		$P_{12}(J)$		$Q_{12}(J)$		$P_{13}(J)$		$Q_{13}(J)$		$P_{23}(J)$	
2							31 791.3497	0.0080	31 794.4562	− 0.0036		
3			31 795.8146	0.0047			31 787.3890	0.0065	31 792.0544	− 0.0070		
4			31 792.4751	− 0.0071	31 798.7244	− 0.0081	31 782.9517	0.0007	31 789.2102	0.0088	31 804.407	− 0.018
5			31 789.1780	0.0009	31 797.0070	− 0.0001	31 778.1504	0.0002	31 785.9824	0.0021	31 799.995	− 0.009
6			31 785.7091	− 0.0005	31 795.1187	− 0.0096	31 773.0288	− 0.0019	31 782.4510	0.0016		
7	31 795.4692	0.0043	31 782.0336	0.0037								

4-3 subband

	$Q_1(J)$		$R_1(J)$		$R_{12}(J)$		$R_{21}(J)$	
4			31 818.8500	0.0008	31 811.7994	− 0.0028	31 851.246	− 0.027
5	31 811.5581	− 0.0215	31 821.2247	0.0029	31 811.9028	0.0139		
6	31 812.0193	− 0.0012	31 823.2791	0.0007	31 811.8392	− 0.0102		
7			31 825.0650	0.0017	31 811.6304	0.0022		
8			31 826.5943	− 0.0020				

TABLE II. Molecular constants for the 0_0^0 band of the $\tilde{A}\,^3E - \tilde{X}\,^3A_2$ system of CH_3N (in cm^{-1}).

Constant	$\tilde{X}\,^3A_2$	$\tilde{A}\,^3E$
T		31 830.913(12)[a]
$a\zeta_e d$		−22.517(16)
λ	0.855 21(66)	−0.2133(78)
$A\zeta_t$		3.2716(63)
$10^4\,\eta_e\zeta_t$		4.3(15)
A	5.61[b]	5.422 90(55)
B	0.929 410(48)	0.844 65(17)
$10^5\,D_K$	7.03[b]	
$10^5\,D_{NK}$		7.2(14)
$10^6\,D_N$	3.76(30)	
ϵ_{aa}		−0.2707(33)
$(\epsilon_{bb}+\epsilon_{cc})/2$	−0.003 29(14)	0.0656(63)
o_1		0.8925(40)
ϵ_1		−0.017 43(75)
h_1		0.001 278(58)
o_2		−0.49(17)
ϵ_{2a}		0.210(87)
ϵ_{2b}		−0.099(20)
h_2		−0.0226(93)

[a] One standard deviation error in parentheses.
[b] Held fixed.

TABLE III. Molecular structure for the $\tilde{X}\,^3A_2$ state of CH_3N.

Parameter	Theory[a]	Experiment
R_{CH} (Å)	1.089	
Θ_{HCH} (deg)	108.7	
R_{CN} (Å)	1.424	1.420

[a] Reference 6.

Methylnitrene has three Jahn–Teller active modes, but in their vibrational analysis Chappell and Engelking[4] found that one ν_6 exhibits the strongest interaction. They determined a Jahn–Teller coupling constant $k^2 = 0.19$ for this mode with $k^2 < 0.02$ for ν_4 and ν_5. Even the ν_6 value of $k^2 = 0.19$ is considered a weak Jahn–Teller effect. Child and Longuet-Higgins[13] use the parameter $D = k^2/2$ to describe the Jahn–Teller effect. In the Appendix of Ref. 13, they give a table relating D to the quenching parameter d, and interpolating the quoted values gives $d = 0.71$ for $D = 0.095$. The projection of the orbital angular momentum, ζ_e, is thus found to be 0.915.

The total projection of the angular momentum for a molecule with a single degenerate mode is given by $\zeta_t = \zeta_e d + \zeta_v(1-d)/2$. For CH_3N with three degenerate modes, this simple expression does not strictly apply, but because $d \simeq 1$ for ν_4 and ν_5, an estimate of the vibronic angular momentum associated with ν_6 can be made giving $\zeta_6 = -0.3$.

Liu *et al.*[14] have recently derived expressions for the Jahn–Teller induced corrections to the parameters in E electronic states, and applied them to the methoxy radical.[15] For the ground $\tilde{X}\,^3A_2$ state, only ϵ_{bb} was determinable with ϵ_{aa} at least a factor of 5 smaller. Contributions to ϵ_{bb} arise in the same fashion as γ for a $^3\Sigma$ state by interaction with excited triplet states. Using the standard pure precession expression, and assuming interaction only with the $\tilde{A}\,^3E$ state, gives $\epsilon_{bb} = 4aB/\Delta E = -0.0038\ cm^{-1}$, in good agreement with the measured value of $-0.0033\ cm^{-1}$. Contributions to ϵ_{aa} come only from excited $^3A_1$ states of which none are known. No theoretical calculations of higher lying triplets are available for CH_3N but for the isovalent NH radical, the first $^3\Sigma^+$ state ($= {}^3A_1$ for CH_3N) is predicted to be repulsive with a vertical excitation energy $> 70\,000\ cm^{-1}$.[16] Hence, ϵ_{aa} for the $\tilde{X}\,^3A_2$ state is expected to be very small and indeed this term was too small to determine experimentally.

For the $\tilde{A}\,^3E$ state, ϵ_{bb} should be equal in magnitude but opposite in sign to ϵ_{bb} for the ground state assuming no other contributions. However, ϵ_{bb} for the $\tilde{A}\,^3E$ state is much larger, suggesting interactions with other unknown excited states. For ϵ_{aa} in the $\tilde{A}\,^3E$ state contributions due to the Jahn–Teller interaction can occur. Following the same procedure as Liu *et al.*[14,15] gives $\epsilon_{aa} = -0.47\ cm^{-1}$ in reasonable accord, considering the approximations required, with the measured value of $\epsilon_{aa} = -0.27\ cm^{-1}$.

CONCLUSION

The $\tilde{A}\,^3E - \tilde{X}\,^3A_2$ transition of methylnitrene has been fully analyzed for the first time. Unfortunately, little extra structural information could be determined, although it is clear that experiment and the highest level theory now agree to within the error of the measurements. Further analysis of deuterated methylnitrene remains to be done. In addition, emission spectra to several excited vibrational levels of the ground state are available.

ACKNOWLEDGMENTS

We appreciate the expert technical assistance of J. Wagner and G. Ladd in obtaining the spectra at Kitt Peak. The National Solar Observatory is operated by the Association of Universities for Research in Astronomy Inc., under contract with the National Science Foundation. This research was supported by the Astronautics Laboratory (now Phillips Laboratory, Propulsion Directorate), Edwards Air Force Base, California.

APPENDIX: HAMILTONIAN AND MATRIX ELEMENTS FOR $A\,^3E$ ELECTRONIC STATE

Hamiltonian terms diagonal in K

$$H = H_{SO} + H_{COR} + H_{ROT} + H_{CD} + H_{SR} + H_{SS},$$

$$H_{SO} + H_{COR} = aL_zS_z - 2AN_z(L_z + G_z),$$

$$H_{ROT} = AN_z^2 + B(N_x^2 + N_y^2),$$

$$H_{CD} = -D_N N^4 - D_{NK} N^2 N_z^2 - D_K N_z^4,$$

$$H_{SR} = \epsilon_{aa} N_z S_z + (\epsilon_{bb} + \epsilon_{cc})(N_+ S_- + N_- S_+)/4,$$

$$H_{SS} = 2\lambda(S_z^2 - S^2/3).$$

Interaction terms between levels differing in K

$$H' = h_1[\Lambda^2_- N^2_+ + \Lambda^2_+ N^2_-] + h_2[\Lambda^2_- (N_z N_- + N_- N_z) + \Lambda^2_+ (N_z N_+ + N_+ N_z)]$$
$$+ o_1[\Lambda^2_- S^2_+ + \Lambda^2_+ S^2_-] + o_2[\Lambda^2_- (S_z S_- + S_- S_z) + \Lambda^2_+ (S_z S_+ + S_+ S_z)]$$
$$+ \epsilon_1[\Lambda^2_- N_+ S_+ + \Lambda^2_+ N_- S_-] + \epsilon_{2a}[\Lambda^2_- (N_z S_- + S_- N_z) + \Lambda^2_+ (N_z S_+ + S_+ N_z)]$$
$$+ \epsilon_{2b}[\Lambda^2_- (S_z N_- + N_- S_z) + \Lambda^2_+ (S_z N_+ + N_+ S_z)].$$

Diagonal matrix elements

$$\langle JKP\Sigma; \pm | H | JKP\Sigma; \pm \rangle = a\zeta_e d\Sigma - 2AK\zeta_t + 2\lambda(\Sigma^2 - 2/3) + \epsilon_{aa} K\Sigma + 1/2(\epsilon_{bb} + \epsilon_{cc})(2 - \Sigma^2)$$
$$+ (A - B)K^2 + B[J(J+1) - 2(K+\Sigma)\Sigma + 2]$$
$$- D_K K^4 - D_{NK}[J(J+1) - 2(K+\Sigma)\Sigma + 2]K^2$$
$$- D_N[(J(J+1))^2 - 4\Sigma K J(J+1) + (8 - 6\Sigma^2)J(J+1)$$
$$- (4 - 6\Sigma^2)K^2 - 2\Sigma K + 4(1 - \Sigma^2)],$$

where

$$\zeta_e d \equiv \langle \zeta | L_z | \zeta \rangle$$

and

$$\zeta_t \equiv \langle \zeta | L_z + G_z | \zeta \rangle.$$

Spin-uncoupling

$$\langle JK,P+1,\Sigma+1; \pm | H | JKP\Sigma; \pm \rangle$$
$$= -[B - 2D_N[J(J+1) + K - 1 - 2\Sigma] - D_{NK}K^2$$
$$- (\epsilon_{bb} + \epsilon_{cc})/4]$$
$$\times [2J(J+1) - 2(K+\Sigma)(K+\Sigma+1)]^{1/2},$$

$$\langle JK,P+2,\Sigma+2; \pm | H | JKP\Sigma; \pm \rangle$$
$$= -2D_N[J(J+1) - K(K-1)]^{1/2}[J(J+1)$$
$$- K(K+1)]^{1/2}.$$

Elements off-diagonal in K

$$\langle J, -K+2, -P+2, -\Sigma; \pm | H' | JKP\Sigma; \pm \rangle$$
$$= \pm(-1)^{J-K+1} h_1[J(J+1) - (K+\Sigma-1)(K$$
$$+ \Sigma - 2)]^{1/2}[J(J+1)$$
$$- (K+\Sigma)(K+\Sigma-1)]^{1/2},$$

$$\langle J, -K+2, -P+1, -\Sigma-1; \pm | H' | JKP\Sigma; \pm \rangle$$
$$= \pm(-1)^{J-K+1}(\epsilon_1 - 2h_1)$$
$$\times [2J(J+1) - 2(K+\Sigma)(K+\Sigma-1)]^{1/2},$$

$$\langle J, -K+2, -P, -\Sigma-2; \pm | H' | JKP\Sigma; \pm \rangle$$
$$= \pm(-1)^{J-K+1} 2(o_1 + h_1 - \epsilon_1),$$

$$\langle J, -K-1, -P-1, -\Sigma; \pm | H' | JKP\Sigma; \pm \rangle$$
$$= \pm(-1)^{J-K}[h_2(2K+1) + 2\epsilon_{2b}\Sigma]$$
$$\times [J(J+1) - (K+\Sigma)(K+\Sigma+1)]^{1/2},$$

$$\langle J, -K-1, -P, -\Sigma+1; \pm | H' | JKP\Sigma; \pm \rangle$$
$$= \pm(-1)^{J-K}[(\epsilon_{2a} - h_2)(2K+1)$$
$$+ (o_2 - \epsilon_{2b})(2\Sigma - 1)](2)^{1/2}.$$

[1] P. G. Carrick and P. C. Engelking, J. Chem. Phys. **81**, 1661 (1984).
[2] J. Demuynck, D. J. Fox, Y. Yamaguchi, and H. F. Schaefer III, J. Am. Chem. Soc. **102**, 6204 (1980).
[3] P. G. Carrick, C. R. Brazier, P. F. Bernath, and P. C. Engelking, J. Am. Chem. Soc. **109**, 5100 (1987).
[4] E. L. Chappell and P. C. Engelking, J. Chem. Phys. **89**, 6007 (1988).
[5] R. F. Ferrante, J. Chem. Phys. **86**, 25 (1987); **94**, 4678 (1991).
[6] Y. Xie, G. E. Scuseria, B. F. Yates, Y. Yamaguchi, and H. F. Schaefer III, J. Am. Chem. Soc. **111**, 5181 (1989).
[7] I. Wysong Milkman, J. C. Choi, J. L. Hardwick, and J. T. Moseley, Rev. Sci. Instrum. **59**, 508 (1988).
[8] Y. Endo, S. Saito and E. Hirota, J. Chem. Phys. **81**, 122 (1984).
[9] C. R. Brazier and P. F. Bernath, J. Chem. Phys. **91**, 4548 (1989).
[10] G. Graner, Mol. Phys. **31**, 1833 (1976).
[11] C. H. Townes and A. L. Schawlow, *Microwave Spectroscopy* (Dover, New York, 1975), p. 54.
[12] C. R. Brazier, R. S. Ram, and P. F. Bernath, J. Mol. Spectrosc. **120**, 381 (1986).
[13] M. S. Child and H. C. Longuet-Higgins, Proc. R. Soc. London, Ser. A **254**, 259 (1961).
[14] X. Liu, L. Yu, and T. A. Miller, J. Mol. Spectrosc. **140**, 112 (1990).
[15] X. Liu, S. C. Foster, J. M. Williamson, L. Yu, and T. A. Miller, Mol. Phys. **69**, 357 (1990).
[16] J. Kouba and Y. Ohrn, J. Chem. Phys. **52**, 5387 (1970).